

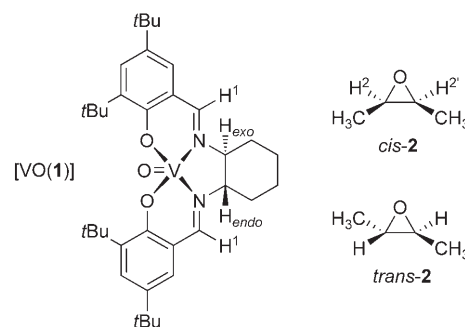
Discrimination of Geometrical Epoxide Isomers by ENDOR Spectroscopy and DFT Calculations: The Role of Hydrogen Bonds**

Damien M. Murphy,* Ian A. Fallis,* David J. Willock,* James Landon, Emma Carter, and Evi Vinck

In the last two decades metal complexes of Schiff base salen-type (salen = *N,N'*-bis(3,5-*tert*-butylsalicylidene)-1,2-cyclohexane diamine) ligands have evolved to become one of the most significant and broadly applied classes of homogenous catalysts.^[1] Among the most useful transformations reported are those featuring epoxides as substrates or products. Key examples include olefin oxidation,^[2,3] the deracemization of *meso* epoxides^[4] and epoxy alcohols,^[5] hydrolytic kinetic resolution,^[6] and stereospecific polymerization^[7] of racemic epoxides. Despite the importance of such reactions, the mode of epoxide interaction with the catalysts is difficult to detect owing to the inherent reactivity of the system.

Herein we demonstrate how electron nuclear double resonance (ENDOR) spectroscopy, combined with density functional theory (DFT) calculations, can be used to visualize even the most subtle and weak epoxide–metallo-salen interactions. We have used the chiral complex [VO(1)] (Scheme 1) as a spectroscopically accessible d¹ probe to examine the stereochemistry of this weak epoxide–metallo-salen interaction in solution, without the risk of epoxide ring opening reactions or polymerizations associated with more strongly Lewis acidic systems. Furthermore, we show how weak hydrogen bonds are responsible for controlling the stereochemistry of the epoxide–metallo-salen adducts.

We examined the interactions of racemic [VO(1)] with *cis* and *trans* isomers of 2,3-epoxybutane (*cis*-2 and *trans*-2) as a means of differentiating the binding mode of these geometrical epoxide isomers with [VO(1)]. This system is important because of the differences in reactivity between *cis/trans* epoxides, and *cis/trans* alkenes. For example, [CrCl(1)] has been shown to deracemize *meso* epoxides, whereas [MnCl(1)] is an effective oxidation catalyst specifi-



Scheme 1. Structure of the vanadyl–salen complex [VO(1)] and the model epoxide substrates. Note the pyramidalization at the vanadium center.

cally for *cis* alkenes. The reactivity patterns of the former suggest well defined transition states in which *cis* epoxides are bound and activated by interaction with the chiral [CrCl(1)] complex. For [MnCl(1)], an epoxide bound complex has been observed in the solid state,^[8] but this predissociation reaction intermediate has hitherto been unobserved in solution.

The continuous-wave EPR (CW EPR) spectra of *rac*-[VO(1)] dissolved in *trans*-2 and *cis*-2 are shown in Figure 1. These spectra were simulated with a rhombic *g* value and a ⁵¹V hyperfine tensor (Table 1). The EPR parameters for [VO(1)] dissolved in *cis*-2 are slightly different relative to those for *trans*-2. Axial coordination of the *cis* epoxide (*cis*-2) to the [VO(1)] complex can be evidenced by the small changes, specifically the reduction of $|A_z|$ and the decrease of g_x relative to that observed for [VO(1)] dissolved in toluene. These subtle changes to g_x and $|A_z|$ are analogous to

[*] Dr. D. M. Murphy, Dr. I. A. Fallis, Dr. D. J. Willock, J. Landon, Dr. E. Carter
School of Chemistry, Cardiff University
Main Building, Park Place, Cardiff, CF10 3AT (UK)
Fax: (+44) 29-874-030
E-mail: willockdj@cardiff.ac.uk
E-mail: fallis@cardiff.ac.uk
E-mail: murphydm@cardiff.ac.uk

E. Vinck
SIBAC laboratory—Department of Physics, University of Antwerp
Universiteitsplein 1, 2610 Wilrijk (Belgium)

[**] We thank the EPSRC for support (EP/E030122), the Cardiff Institute of Tissue Engineering and Repair (CITER), and JREI (JR99BAPAEQ) for a 20 processor Compaq SC cluster at the Rutherford Appleton Laboratory.

Supporting information for this article is available on the WWW under <http://www.angewandte.org> or from the author.

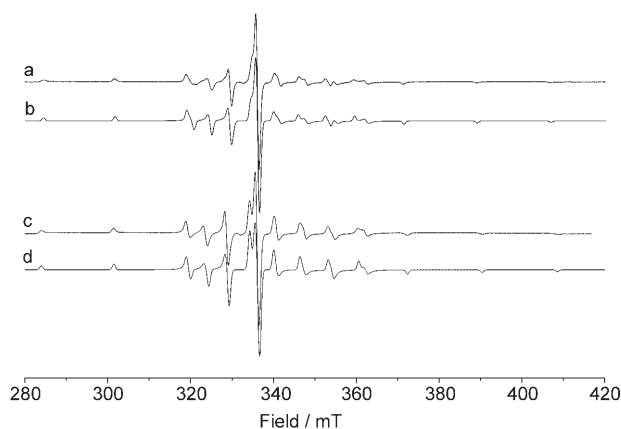


Figure 1. X-band CW EPR spectra (10 K) of *rac*-[VO(1)] dissolved in a) *cis*-2 and c) *trans*-2. Respective simulations shown in (b) and (d).

Table 1: EPR spin Hamiltonian parameters for *rac*-[VO(1)] dissolved in toluene, *trans*-2, and *cis*-2.

Solvent	$g_x^{[a]}$	$g_y^{[a]}$	$g_z^{[a]}$	A_x [MHz] ^[b]	A_y [MHz] ^[b]	A_z [MHz] ^[b]
toluene	1.9828	1.9805	1.9525	−172	−161	−487
<i>trans</i> -2	1.9828	1.9805	1.9525	−172	−161	−487
<i>cis</i> -2	1.9820	1.9805	1.9525	−170	−160	−480

[a] ± 0.004 , [b] ± 2 MHz.

the trends observed in other axially ligated vanadyl complexes.^[9] The EPR spectrum observed for [VO(1)] in *trans*-2 is identical to that found for the toluene case, suggesting no coordination of the bulkier *trans*-2 to the complex.

The [VO(1)]–epoxide interaction was then examined by DFT calculations at the BHandHLYP level. Given that [VO(1)] and *trans*-2 are chiral moieties, calculations on the diastereomeric adducts (*R,R'*)-[VO(1)]–(*R,R'*)-*trans*-2 and (*R,R'*)-[VO(1)]–(*S,S'*)-*trans*-2 were required. The salen N₂O₂ atoms co-ordinating the V center and the chiral centers of (*R,R'*)-[VO(1)] are shown in Figure 2. This work revealed, unexpectedly, that the closest approach of the epoxide to [VO(1)] is between the epoxide oxygen atom (O_{ep}) and the methine proton H^{exo} of the cyclohexyl group, as opposed to V...O_{ep}. The C–H^{exo}...O_{ep} calculated distances (Table 2) range from 2.36 to 2.48 Å, values typical of hydrogen-bond interactions with C–H donors,^[10] whereas the V...O_{ep} distances are well outside the range of any typical V–O bonds.

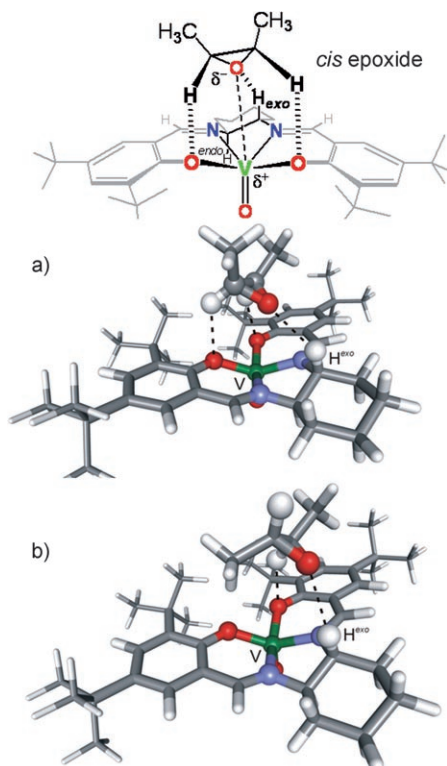

Figure 2: DFT structures of (*R,R'*)-[VO(1)] adducts with a) *cis*-2 and b) (*R,R'*)-*trans*-2. The key atoms are illustrated as spheres. The scheme illustrates the hydrogen bonding (dashed lines) in the *cis*-2 case and the electrostatic interactions are not shown.

Table 2: DFT (BHandHLYP/6-31G(d,p)) calculated structural parameters and energies for epoxides interacting with (*R,R'*)-[VO(1)].

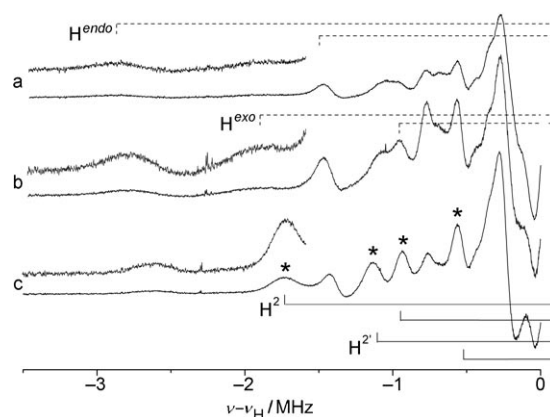
Epoxide	V...O _{ep} ^[a] [Å]	C–H ¹ ...O _{ep} [Å]	O _{ep} ...V=O [°]	θ_{plane} ^[b] [°]	E_{el} [kJ mol ^{−1}]
<i>cis</i> -2	3.504	2.469	168	32	−18
(<i>R,R'</i>)- <i>trans</i> -2	4.156	2.480	160	42	−13
(<i>S,S'</i>)- <i>trans</i> -2	4.048	2.362	162	39	−12

[a] O_{ep} = epoxide oxygen atom; [b] θ_{plane} = angle between the normal to the plane of the epoxide ring and the V=O direction.

The interaction energy (E_{int}) between each epoxide and (*R,R'*)-[VO(1)] was calculated as the difference between the adduct energy and the sum of the isolated energies of the optimized structures. Basis-set superposition error corrections were applied by using the counterpoise method. In all three cases, similar values of E_{int} were found (ca. −18 kJ mol^{−1}). However, the electrostatic contribution to E_{int} (E_{el}) was estimated by a distributed multipole analysis for each epoxide and (*R,R'*)-[VO(1)], and both of the *trans* epoxides (*R,R'* and *S,S'*) show a smaller E_{el} component relative to *cis*-2 (Table 2). In particular, a more favorable C–H^{exo}...O_{ep} hydrogen-bond interaction is found for *cis*-2 than for *trans*-2 (see the Supporting Information). Two additional hydrogen bonds also exist between the epoxide protons 2,2' of *cis*-2 and each of the two oxygen atoms of the salen ligand (Scheme 1). Only one of these hydrogen bonds occurs between *trans*-2 and [VO(1)], since one of the nonpolar methyl groups now points towards the salen oxygen atom (Figure 2).

To confirm the DFT model, ¹H ENDOR spectra for *rac*-[VO(1)] dissolved in [D₈]toluene, *trans*-2, and *cis*-2 were recorded (Figure 3 a–c). For the purposes of reproducibility, ENDOR spectra were measured with (*R,R'*)-[VO(1)] and (*S,S'*)-[VO(1)] and found to be identical.

The spectra are complicated by the presence of superimposed peaks from both ligand and epoxide protons. Identification of the epoxide peaks (labeled * in Figure 3) is not improved by using the subtracted spectrum, as other ligand peaks (H^{exo} and H^{endo}) are distorted upon epoxide


Figure 3: X-band ¹H ENDOR spectra (10 K) for *rac*-[VO(1)] dissolved in a) toluene, b) *trans*-2, and c) *cis*-2 and recorded at the observer position $g = g_{\perp}$. Only the low-frequency components of the spectra, plotted as $\nu - \nu_H$, are shown. The epoxide derived peaks are labeled *.

binding. However, we have previously shown,^[11] by ENDOR spectroscopy and DFT calculations, that the largest proton couplings observable in [VO(**1**)] are due to: 1) the cyclohexyl methine protons (H^{endo} and H^{exo} in Scheme 1, $H_{\text{methine}} \cdots \text{VO}$ distances of 3.023 Å and 3.437 Å), 2) the imine protons (H^{I} , $H_{\text{imine}} \cdots \text{VO}$ distance of about 4.0 Å), and 3) the “inner” *tert*-butyl groups ($H_{\text{butyl}} \cdots \text{VO}$ distance of between 3.43 and 4.05 Å). In [VO(**1**)], the differences in the $H \cdots \text{VO}$ distance for the two methine protons is due to the significant pyramidalization of the VO moiety above the N_2O_2 ligand plane, whereas the range in proton distances for the *tert*-butyl groups is due to the presence of rotamers.

As seen in Figure 3c, couplings to H^{exo} and H^{endo} decrease after binding *cis*-**2**. The decrease in H^{endo} coupling is due to the slight decrease in pyramidalization of VO after *cis*-**2** binding, typical of axial ligation in VO complexes.^[12] The decrease in H^{exo} is due to hydrogen bonding with the epoxide, as evidenced by a slight lengthening of the $H^{\text{exo}} \cdots \text{VO}$ distance that arises from torsional changes within the ligand framework. This observation corroborates the DFT results.

The labeled (*) peaks in Figure 3c originate from the protons of *cis*-**2**, since they are absent in the toluene case (Figure 3a). Two distinct proton couplings (Table 3) were

Table 3: ^1H ENDOR couplings and DFT-derived distances for H^2 and $H^{2'}$ (see Scheme 1 for labels) in the *cis*-**2**-[VO(**1**)] adduct.

	A_{\parallel}^{a}	A_{iso}	A_1	A_2	A_3	R [Å] ^b	θ_{H} [°]	R [Å] ^c
H^2	4.47	−0.10	−1.85	−2.80	4.38	3.26	55	3.30
$H^{2'}$	2.70	−0.10	−1.10	−1.80	2.60	3.86	60	3.97

[a] All A values given in MHz (± 0.05); A_{\parallel} = dipolar hyperfine coupling; [b] R distance derived by ENDOR spectroscopy; [c] R distance derived by DFT calculations.

identified by simulations of the ENDOR spectra (see the Supporting Information). The $\text{VO} \cdots H_{\text{epoxide}}$ distances were calculated by using a simple point-dipole approximation and, by reference to the DFT-derived model, were found to originate from the 2,2' protons of *cis*-**2**. By comparison, the ^1H ENDOR spectrum of [VO(**1**)] dissolved in *trans*-**2** is very similar to that observed using toluene, with only a slight broadening of the peaks attributed to the different interactions between [VO(**1**)] and toluene or the more polar epoxide. Nevertheless, the epoxide derived peaks found in Figure 3c are clearly absent in Figure 3b, with good agreement between the DFT structural model and ENDOR spectrum, proving that [VO(**1**)] selectively binds *cis*-**2** in preference to *trans*-**2**. The selectivity towards *cis*-**2** was confirmed in a competition experiment using a 1:1 mixture of *cis*-**2** and *trans*-**2**, producing an identical ENDOR spectrum to that of the pure *cis*-**2** case (Figure 3c). Similar results were obtained upon dilution with toluene (see the Supporting Information).

To put these results into a broader context, it should be noted that in the epoxidation of alkenes by [MnCl(**1**)], the mode of oxygen-atom transfer has long been a subject of debate.^[13] We suggest that *cis*-**2**-[VO(**1**)] adducts are good models for the catalyst–substrate predissociation complexes in this reaction. Herein, we have shown that the adduct is stabilized by a weak electrostatic $\text{V}^{\delta+} \cdots \text{O}_{\text{ep}}^{\delta-}$ interaction augmented by multiple hydrogen bonds. Crucially, these hydrogen bonds facilitate the overall orientation of the epoxide between the metal center and the chiral salen backbone. Furthermore, such an arrangement is favorable in the more symmetrical *cis*-**2**, but sterically unfavorable in the *trans*-**2**. Jacobsen and co-workers have shown that [MnCl(**1**)] complexes, bearing electron-donating substituents, afford the best enantioselectivities,^[2] and we suggest that these electron-rich ligands would also show enhanced hydrogen-bond interactions to the phenoxide donors. These hydrogen bonds may help to orient transition-state intermediates, and may therefore be important in directing the stereochemical outcome of this important reaction.

Received: August 3, 2007

Revised: November 16, 2007

Published online: January 15, 2008

Keywords: chirality · density functional calculations · ENDOR spectroscopy · epoxides · EPR spectroscopy

- [1] T. P. Yoon, E. N. Jacobsen, *Science* **2003**, 299, 1691–1693.
- [2] M. Palucki, N. S. Finney, P. J. Pospisil, M. L. Guler, T. Ishida, E. N. Jacobsen, *J. Am. Chem. Soc.* **1998**, 120, 948–954.
- [3] E. M. McGarrigle, D. G. Gilheany, *Chem. Rev.* **2005**, 105, 1563–1602.
- [4] L. E. Martinez, J. L. Leighton, D. H. Carsten and E. N. Jacobsen, *J. Am. Chem. Soc.* **1995**, 117, 5897–5898.
- [5] M. H. Wu, K. B. Hansen, E. N. Jacobsen, *Angew. Chem.* **1999**, 111, 2167–2170; *Angew. Chem. Int. Ed.* **1999**, 38, 2012–2014.
- [6] M. Tokunaga, J. F. Larrow, F. Kakiuchi, E. N. Jacobsen, *Science* **1997**, 277, 936–938.
- [7] K. L. Peretti, H. Ajiro, C. T. Cohen, E. B. Lobkovsky, G. W. Coates, *J. Am. Chem. Soc.* **2005**, 127, 11566–11567.
- [8] T. Hashihayata, T. Punniyamurthy, R. Irie, T. Katsuki, M. Akita, Y. Moro-oka, *Tetrahedron* **1999**, 55, 14599–14610.
- [9] B. Kirste, H. van Willigen, *J. Phys. Chem.* **1982**, 86, 2743–2749.
- [10] a) G. A. Jeffrey, *An Introduction to Hydrogen Bonding*, Oxford University Press, Oxford, **1997**; b) L. Lo Presti, R. Soave, R. Destro, *J. Phys. Chem. B* **2006**, 110, 6405–6414.
- [11] I. A. Fallis, D. M. Murphy, D. J. Willock, R. J. Tucker, R. D. Farley, R. Jenkins, R. R. Strevens, *J. Am. Chem. Soc.* **2004**, 126, 15660–15661.
- [12] R. J. Tucker, I. A. Fallis, R. D. Farley, D. M. Murphy, D. J. Willock, *Chem. Phys. Lett.* **2003**, 380, 758–766.
- [13] M. P. Feth, C. Bolm, J. P. Hildebrand, M. Köhler, O. Beckmann, M. Baur, R. Ramamomjisoa, H. Bertagnolli, *Chem. Eur. J.* **2003**, 9, 1348–1359, and references therein.